Calibration of coherence imaging spectroscopy using spectral line sources

Calibration of Coherence Imaging Spectroscopy using spectral line sources.

Kenji UEDA,[1, a)] Masaki NISHIURA,[1,2] Naoki KENMOCHI,[2] Zensho YOSHIDA,[1,2] Kaori NAKAMURA,[1]

[1] *Graduate School of Frontier Sciences, The University of Tokyo, 5-1-5 Kashiwanoha, Kashiwa, Chiba, 277-8561, Japan*
[2] *National Institute for Fusion Science, 322-6 Oroshi-cho, Toki, Gifu, 509-5292, Japan*

(Presented XXXXX; received XXXXX; accepted XXXXX; published online XXXXX)
(Dates appearing here are provided by the Editorial Office)

Coherence imaging spectroscopy (CIS) measures the two-dimensional profiles of both ion temperature and ion velocity in plasmas. The interferometric technique is realized by a certain relation between a phase and a wavelength of light emerging from the birefringent crystal. The calibration for the CIS system requires monochromatic and tunable light sources near He II line (468.6 nm) or C III line (465 nm) where the CIS measures. In this research, the CIS system has been upgraded by implementing an electron multiplier CCD (EM-CCD) and a CIS cell. A monochromator validates the linearity of the phase relation on the wavelength near the He II line. As an in-situ calibration at Ring Trap 1 (RT-1) plasma device, two spectral lines of Ti and Zn lamps obtain the accurate dispersion function of phase. It is found that the simple method with two spectral lines is reliable and sufficient for the calibration.

I. INTRODUCTION

Doppler spectroscopy is widely applied to diagnose phenomena as a non-contact method. Since the Doppler effect influences a width and a shift of a spectral line, the spectral analysis gives us valuable information on particle behaviors in a medium. To understand self-organized plasmas in a dipole confinement device Ring-Trap 1 (RT-1), Doppler spectroscopy is utilized in high-beta plasmas to study the heat and particle transports, which imitate a planetary magnetospheric plasma in the laboratory[1,2]. To understand the role of ion flow in self-organized plasmas, coherence imaging spectroscopy (CIS) has been developed in the RT-1[3].

CIS is a powerful tool for Doppler spectroscopy, and measures the two-dimensional images of ion temperature and flow velocity, which are more informatic and cost effective compared with spectroscopic measurements with a grating spectrometer. The pioneering work for CIS has been carried out by J. Howard et al.[4-6], and the CIS has been successfully demonstrated on plasma and thermonuclear fusion devices such as MAST[7], DIII-D[8-9], ASDEX-U[10], and W7-X[11,12]. While those CIS systems are optimized for their purposes, the fundamental principle is based on the polarimetric spectroscopy realized by means of a birefringent crystal. Our previous paper has reported the development of the simple CIS system[3]. The enhancement of ion temperature and toroidal flow velocity has been observed clearly by applying the ion cyclotron slow-wave heating (ICH) in the RT-1. In that case, the CIS diagnostics contributes to the visualization of the effect of ion heating on the spatial profile[13].

Calibration of CIS requires a light source with a wavelength close to the spectral line of interest. Spectral lamps[8,10] or tunable continuous wave lasers[7,9,11] are mainly used as light sources for calibration. When the former is used, the spectral lines of the light source do not match the emission lines of the plasma, so the phase of CIS must be extrapolated[8]. When using the latter, the dispersion relation of the phase can be directly measured by sweeping the wavelength of the light source[11]. In this paper, we focus on the upgraded system for field widening and sensitivity and the calibration methods with a monochromator and two light sources. The former method with the monochromator verifies the phase linearity of birefringent crystals as a function of the wavelength. The latter method, as practical usage, introduces two light sources of Zinc and Titanium to calibrate the CIS system cost-effectively in between discharges, after the CIS system is implemented in the RT-1.

II. MEASUREMENT PRINCIPLE OF CIS

A CIS system is a kind of interferometer realized by birefringent crystals and polarization optics. The measured interferogram is provided by optical autocorrelation with exploiting refractive indices which arise from anisotropy of a birefringent crystal. A signal of interferogram S is generally expressed as,[4]

$$S = I_0(1 + \zeta \cos\phi), \tag{1}$$

[a)] ueda.kenji19@ae.k.u-tokyo.ac.jp

where I_0 is the intensity of the brightness, ζ is the contrast of the fringe, and ϕ is the phase difference, which depends on the wavelength. CIS diagnoses an ion temperature and flow velocity, which comes from Doppler broadening and shift in plasmas. Since the observed shift of a spectral line is small enough, ϕ can be linearized around the spectral line of interest λ_0 as $\phi \simeq \phi_0 + \hat{\phi}_0\ (\lambda - \lambda_0)/\lambda_0$. Here, ϕ_0 is equal to a phase when the velocity due to the Doppler shift is zero. $\hat{\phi}_0$ is a value determined by the dispersion relation of the phase. Applying the above approximation into the Doppler broadening and Doppler shift, the expression for S can be written as,

$$S = I_0 \left(1 + \zeta_I \exp\left(\frac{-T_D}{T_c}\right) \cos\left(\phi_0 + \hat{\phi}_0 \frac{V_D}{c}\right)\right), \qquad (2)$$

where ζ_I is an instrument contrast caused by all dispersions except phase dispersion. The characteristic temperature T_c is equal to $2mc^2/k_B\hat{\phi}_0$, which is obtained for a Maxwellian distribution function. T_D and V_D are the temperature and the velocity of particles due to the Doppler effect, respectively.

In the case of CIS, S can be acquired as the image, or in other words, as a two-dimensional function like $S(x, y)$. $I_0(x, y)$, $\zeta(x, y)$, *and* $\phi(x, y)$ can be extracted naively from $S(x, y)$ if a technique of Fourier analysis can be effectively used. To obtain ion temperature and ion flow velocity from observable quantities such as ζ and ϕ, intrinsic quantities of device, ζ_I, ϕ_0, and $\hat{\phi}_0$, need to be known as two-dimensional functions in advance. Acquiring these values requires certain calibration techniques using monochromatic light sources with high wavelength accuracy.

III. EXPERIMENTAL SETUP OF THE CIS SYSTEM

The CIS system in the RT-1 has been developed[3]. The whole system of the CIS is shown in Fig. 1. The components comprise an electron multiplier CCD (EM-CCD) camera, a CIS cell, an interference filter, and three lenses (an objective lens, a collimating lens, and an imaging lens). The CMOS camera in the previous system was replaced with the EM-CCD camera (PhotonMAX 512B from the Princeton Instruments), which improves sensitivity to the quantity of light. The sensor of this camera has 512×512 image pixels and an 8.2×8.2-mm imaging area. The objective lens collects an emission light from the plasmas. Once imaged at a first focal plane, the rays are collimated and transmit in parallel between the collimating lens and the imaging lens. The interference filter passes the light with a narrow bandwidth of around 1 nm near the spectral line of interest (He II, 468.6 nm). The polarized light is autocorrelated in the CIS cell. The imaging lens forms the interferogram at a second focal plane, where the sensor locates.

The CIS cell is composed of a delay plate, a displacer plate, and polarizers to give an interferogram. The arrangements in the two cases are shown in Fig. 2. The conventional CIS cell in the RT-1 CIS system3 used a pair of the delay plate and the displacer plate (case 1), which are α-BBO birefringent crystals with the optical axes of parallel and 45 degrees to the incident plane, respectively. The thicknesses of the delay plate with 15 mm and the displacer plate with 3 mm are designed based on the plasma parameters of the RT-1 measured by a grating spectrometer. Case 2 of the CIS cell, where a pair of delay and displacer plate and the half-wave plate is additionally mounted, is applied in expectation of improving measurement accuracy. For the half-wave plate's function of exchanging a phase of ordinary and extraordinary rays, an asymmetric component of $\phi(x, y)$ is canceled out and the fringe pattern becomes uniform. The improved effect on the fringe pattern in this system is calculated and is tested by a monochromatic light source. The details are described in the latter section.

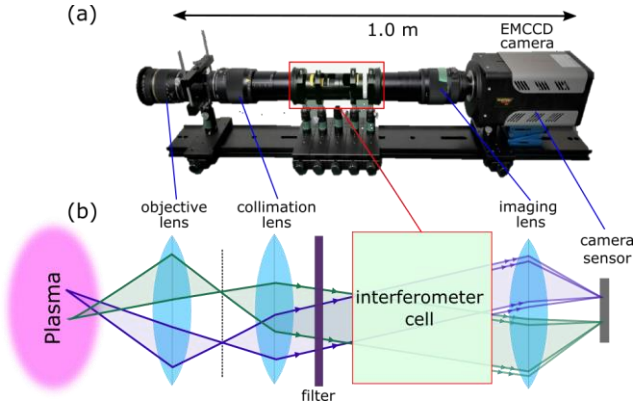

FIG. 1. A photo of RT-1 CIS system (a) and its conceptual schematic (b). The green and violet beams represent examples of light path through the system. The objective lens (focal length 10-24 mm, F/3.5-4.5) views plasma with a wide angle. The collimation lens and the imaging lens (focal length f = 300 mm) provide a region of parallel ray, where the CIS cell is placed.

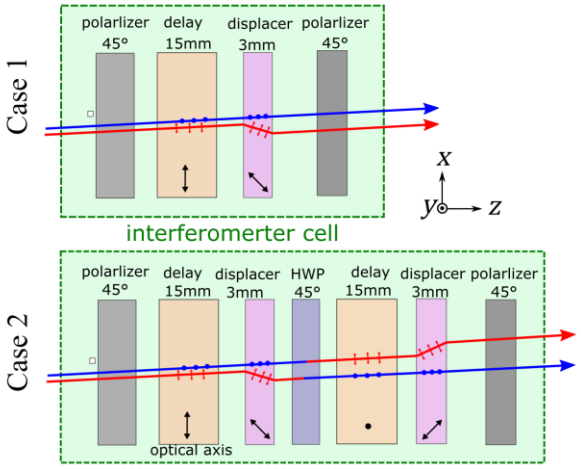

FIG. 2. Arrangement of the CIS cell for two cases. Each plate is deliberately colored for clarity. Blue arrows and red arrows represent ordinary rays and extraordinary rays. Case 1 consists of a pair of the delay plate and the displacer plate. Case 2 consists of two pairs of the delay plate and the displacer plate, and the halfwave plate (HWP). The polarizers are placed at the entrance and exit of the cell for both cases.

IV. ANALYSIS OF INTERFEROGRAM FOR THE CIS

The interferogram on the image sensor for the CIS is calculated by an analytical model. The phase difference ϕ between ordinary and extraordinary waves is formulated by Veiras et al[14] and an application of this formula to a CIS system is well discussed in C. M. Samuell's study[8]. We applied it to two cases in Fig. 2.

A collimated ray with two-dimensional angles (α, δ) is focused on a point (x, y) of the sensor plane, as functions $x = f \cdot \tan\alpha \cos\delta$, and $y = f \cdot \tan\alpha \sin\delta$, where f is the focal length of the imaging lens. Passing through the CIS cell, each ray has a certain amount of phase given $\phi = \sum_{\mathrm{i}} 2\pi\, L_{\mathrm{i}} B_{\mathrm{i}}/\lambda$, where the subscript i indicates the respective plate, L is the effective thickness, λ is the wavelength of incident light in vacuum, and B is the birefringence. According to Veiras' definition, B is a function that depends on the angles of ray, the refractive indices n_e, n_o, and the angle of the optical axis θ, so that the phase image of CIS can be modeled as,

$$\phi(x,y) = \frac{2\pi}{\lambda} \sum_{\mathrm{i}} L_{\mathrm{i}} B(x, y, n_e, n_o, \theta_i)\,. \qquad (3)$$

Refractive indices of crystals are not constant with respect to wavelength so that B becomes a function of λ. $n_e(\lambda)$ and $n_o(\lambda)$ of α-BBO are used from Sellmeier's dispersion equation. As a result of calculation, averages of $\hat{\phi}_0(x,y)/\lambda_0$ are theoretically obtained as -68.6 rad/nm in case 1 and -126 rad/nm in case 2. This means that upgrading from case 1 to case 2 increases the sensitivity of the velocity measurement by a factor of 1.8.

The comparison between theoretical and experimental images of the CIS system in each case of the cell is shown in Fig. 3. The interference fringe pattern seems to be similar between them. On the other hand, the phase difference values are locally more than 6 rad, which is equivalent to a velocity error of 32 km/s. These differences are potentially affected by various parameters such as thickness, refractive index, and focal length, as well as optical alignment, which makes it hard to identify the cause completely.

Here, the error of phase can be reduced comparatively by extrapolating using the following function,

$$\phi(x,y,\lambda) = \phi_0(x,y) + \hat{\phi}_0(x,y) \cdot \left(\frac{\lambda_0}{\lambda} - 1\right), \qquad (4)$$

which can be derived from Eq. 3 by omitting the effect of quadratic dispersion $d^2B/d\lambda^2$. In the approximation of Eq. 4, the residual value of velocity is estimated to be about 0.3 km/s when $\Delta\lambda = \lambda - \lambda_0$ is 1 nm, which is about a tenth smaller than that in the linear approximation.

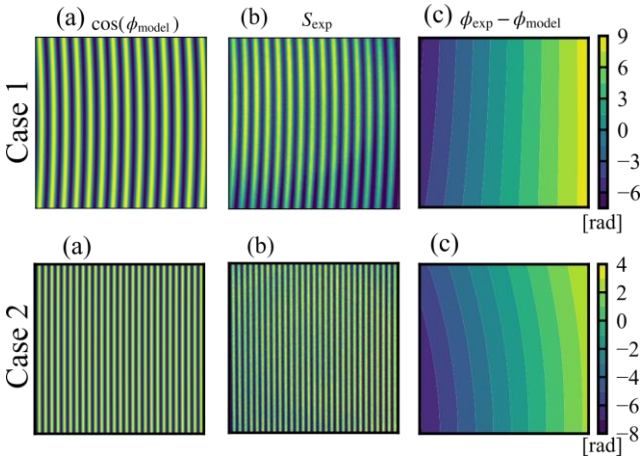

FIG. 3. Fringe patterns of calculation or measurement results. The first row is case 1 and the second row is case2. (a) Images of $\cos\phi(x,y)$ calculated from Eq. 3. (b) Results of measuring uniform light source for calibration with exposure time of 30 s. (c) Difference between model phase and experimental phase

V. MEASUREMENT WITH MONOCHROMATOR

To apply the CIS system to measuring RT-1 plasmas, the phase behavior in the certain wavelength range needs to be experimentally verified once. As a calibration source, the light from a 1/4 m monochromator (MS257 from the Newport) is introduced into the CIS system. The monochromator, which has a rotating diffraction grating controlled by a stepping motor, can output monochromatic light from the light of lamps in the increment of about 0.03 nm. Measured results for case 1 and case 2 are plotted in Fig. 4. As the results of linear fitting, the slopes at case 1 and case 2 are -71.6 rad/nm and -108.3 rad/nm, respectively. These values differ by about 5% and 10% compared to the theoretical values (Chapter 4). These results indicate that the birefringent crystals of α-BBO used in this study have the linear dependence on the wavelength within the measured range.

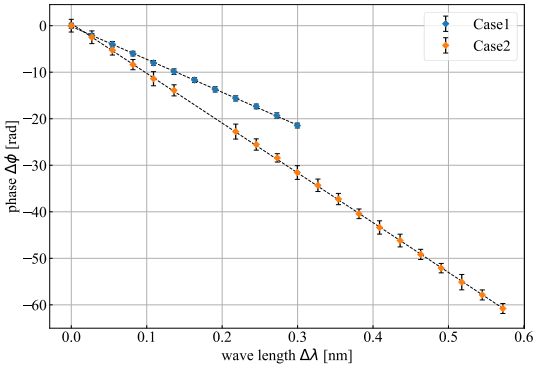

FIG. 4. Results of wavelength vs phase for each case in the CIS measured in the monochromator. The top: the phases are obtained as average of entire image within $\pm\pi$. The bottom: the phases are unwrapped and fitted to linear functions.

VI. CALIBRATION WITH TWO LINES OF SPECTRUM

To perform the absolute calibration of the wavelength of the CIS, hollow cathode lamps which emit the light of the exact and known wavelength are used. Among them, only lamps with exclusive spectral lines close to the line of interest, are required. For the above reason, 468.014 nm[15] line of a Zn lamp are commonly used[8]. Although a calibration with a single lamp is sufficient for ζ_I, a measurement of two or more lines is necessary to calibrate $\phi_0(x,y)$ and $\hat{\phi}_0(x,y)$. The test results (Fig.5) shown that, beside the Zn, it is found that a 468.190 nm[15] line of Ti lamp (L233-22NB from the Hamamatsu Photonics) also satisfies the requirements for a calibration of CIS if an appropriate interferometer filter is used.

$\phi_{\mathrm{Ti}}(x,y)$ and $\phi_{\mathrm{Zn}}(x,y)$ can be obtained experimentally by measuring the spectral lines of Ti and Zn. By substituting λ_{Ti} and λ_{Zn} into Eq. 4 and solving the equation jointly, experimental values of $\phi_0(x,y)$ and $\hat{\phi}_0(x,y)$ can also be obtained. Fig. 6 shows extrapolation of $\phi(\lambda)$ using ϕ_{Ti} and ϕ_{Zn}. The residual from the approximation in Eq. 4 is estimated to be 0.07 km/s when λ_0 is He II line. This amount is acceptable for the RT-1 plasma experiment.

The $\hat{\phi}_0/\lambda_0$ obtained from spectral lines are, on average, -68.0 rad/nm for the case 1 and -124.1 rad/nm for the case 2, respectively. Those values of $\hat{\phi}_0$ indicate agreement within around 1.0 % for the case 1 and within around 1.5 % for the case 2 from the theoretical values (Chapter 4). The errors are due to the assumption of the lens optics and the processing accuracy of the birefringent crystals.

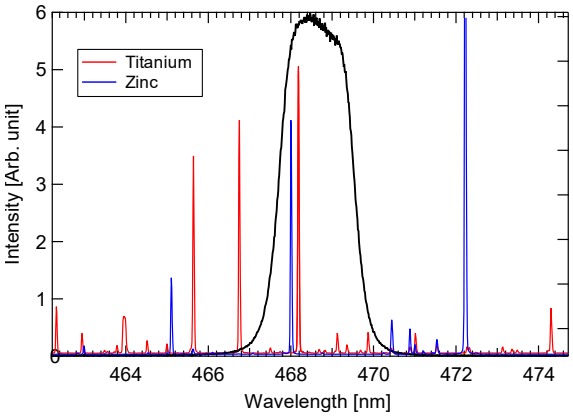

FIG. 5. Spectra of Ti and Zn lamps around 468nm measured with a 1.0 m Czerny–Turner spectrometer. The red line is the spectrum of Ti, the blue line is the spectrum of Zn, and the black line is a transmissivity of the interference filter.

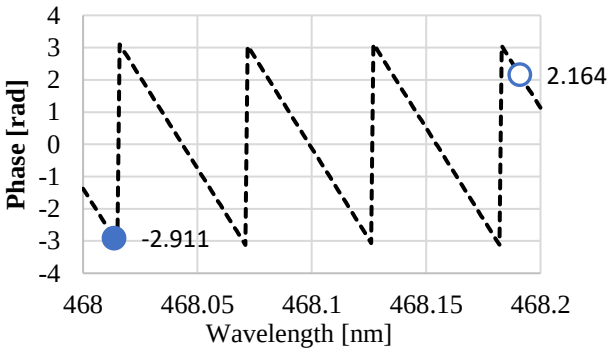

FIG. 6. A phase dependence of wavelength at case 2. A closed circle is phase -2.91 rad at Zn (468.014 nm) and an open circle is phase 2.164 rad at Ti (468.19 nm). A dashed line is extrapolation of $\phi(\lambda)$ through 2 circles.

VII. SUMMARY

The CIS system implemented at the RT-1 has been upgraded for the EM-CCD and the combination of the birefringent crystals to enhance the sensitivity and the fringe uniformity. The interferograms on the CIS system are characterized experimentally by scanning the wavelength near the He II line (468.6 nm) emitted from the monochromator. The linearity of the phase can also be verified from this method instead of using the tunable lasers. The phase ϕ_0 and phase dispersion $\hat{\phi}_0$ are determined by two spectral lines of Zn and Ti for the CIS system. The use of two spectral lines improves the accuracy over the traditional calibration using a spectral lamp. This proposed method is simple and reliable so that it can be an alternative to in-situ calibration in plasma experiments.

VIII. DATA AVAILABILITY

The data that supports the findings of this study are available within the article.

IX. ACKNOWLEDGMENTS

This work was supported by JSPS KAKENHI Grant No.17H01177 and the NIFS Collaboration research program (No. NIFS18KUHL085).

X. REFERENCES

[1] Z. Yoshida, H. Saitoh, Y. Yano, H. Mikami, N. Kasaoka, W. Sakamoto, J. Morikawa, M. Furukawa, and S. M. Mahajan, 2013 Plasma Phys. Control. Fusion 55 014018.
[2] M. Nishiura, Z. Yoshida, H. Saitoh, Y. Yano, Y. Kawazura, T. Nogami, M. Yamasaki, T. Mushiake and A. Kashyap, 2015 Nucl. Fusion 55 053019.
[3]K. Nakamura, M. Nishiura, N. Takahashi, Z. Yoshida, N. Kenmochi, T. Sugata, S. Katsura, and J. Howard, Rev. Sci. Instrum. 89, 10D133 (2018).
[4]J. Howard, C. Michael, F. Glass, and A. Danielsson, 2003 Plasma Phys. Control. Fusion 45 1143.
[5]J. Howard, 2010 J. Phys. B: At. Mol. Opt. Phys. 43 144010.
[6] J. Howard, C. Michael, H. Chen, R. Lester, A. Thormana, and J. Chungb, 2015 JINST 10 P09023.
[7]S S. A. Silburn, J. R. Harrison, J. Howard, K. J. Gibson, H. Meyer, C. A. Michael, and R. M. Sharples, Rev. Sci. Instrum. 85, 11D703 (2014).
[8]C.M. Samuell, S.L. Allen, W.H. Meyer, and J. Howard., 2017 JINST 12 C08016.
[9] S. L. Allen, C. M. Samuell, W. H. Meyer, and J. Howard, Rev. Sci. Instrum. 89, 10E110 (2018).

[10]D Gradic, O P Ford, A Burckhart, F Effenberg, H Frerichs, R König, T Lunt, V Perseo, R C Wolf, ASDEX Upgrade Team, 2018 Plasma Phys. Control. Fusion 60 084007.
[11] D. Gradic, V. Perseoa, R. König, D. Ennis, the W7-X team, Fusion Eng. Des. Volume 146, Part A, September 2019, Pages 995-998.
[12] V. Perseo, D. Gradic, R. König, O. P. Ford, C. Killer, O. Grulke, D. A. Ennis, and W7-X Team, Rev. Sci. Instrum. 91, 013501 (2020).
[13] M. Nishiura, Z. Yoshida, N. Kenmochi, T. Sugata, K. Nakamura, T. Mori, S. Katsura, K. Shirahata and J. Howard 2019 Nucl. Fusion 59 096005.
[14]F. E. Veiras, L. I. Perez, and M. T. Garea, Applied Optics 49(15):2769-77.
[15]See https://physics.nist.gov/PhysRefData/ASD for NIST atomic spectra database lines.